Proposal for a.c. corrosion process of cathodically protected steel pipelines by analyzing anodic and cathodic coupon current densities

Fumio Kajiyama, Dr.
Tokyo Gas Co., Ltd., 5-20, Kaigan, 1-Chome, Minato-ku, Tokyo, 105-8527, Japan

Abstract

Coupon a.c. current density is a key parameter to evaluate the a.c. corrosion risk of cathodically protected steel pipelines. However, it is not well understood as to how higher coupon a.c. current density increases the a.c. corrosion risk. The paper presents the relationship between coupon a.c. current density and the a.c. corrosion risk of cathodically protected steel pipelines, and addresses a.c. corrosion process by analyzing anodic and cathodic coupon current densities which compose coupon a.c. current density for a single period of 50 Hz.

1 Sound evaluation of the a.c. corrosion risk using coupon a.c. current density

Although there is a controversy about the opinion that the a.c. current density is the primary factor in determining the a.c. corrosion likelihood [1-2], d.c. and a.c. current densities as well as polarized potential are responsible for the corrosion process [3-4]. Since the first incident of a.c. corrosion in the mid 1980's [5], coupons have been used to evaluate the a.c. corrosion likelihood of cathodically protected steel pipelines. When coupon a.c. current density is used for evaluation, it is very important to ascertain the coupon a.c. current density to be that affecting a.c. corrosion. Furthermore, if the maximum value of coupon a.c. current density is significantly higher than the average value, evaluation of the a.c. corrosion risk can be optimistic. Therefore, it is indispensable to avoid this misleading by sound procedure for acquisition of coupon a.c. current density in measuring period particularly in the case of a.c.-electrified railway loading changes.

2 Terms and definitions

The terms and definitions used in this paper are given as described below.

This paper deals with the a.c. corrosion likelihood of cathodically protected steel pipelines at frequency of 50 Hz using coupon technology. The measuring system for evaluation of the cathodic protection level was given by a detailed description in the published papers [6-7].

Coupon potential, $E_{off}(t)$: The coupon-to-electrolyte potential measured between the coupon and the pipe after disconnection of the coupon from the pipe.

Coupon instant-off potential, E_{off}: The coupon potential measured immediately after the coupon is disconnected from the pipe, which closely approximates the potential without IR drop from the protection current and any other current such as a.c. interference current (i.e., the polarized potential). Coupon instant-off potential is obtained from equation (1).

Coupon current, $I(t)$: The current obtained at intervals of 0,1 ms which flows between the coupon and the pipe while the cathodic protection system is continuously operating. Positive values in coupon current indicate the current flowing through electrolyte to the coupon (i.e., cathodic current flowing).

Coupon d.c. current density, $I_{d.c.}$: Using coupon current $I(t)$ for a single period of 50 Hz (i.e., each subunit), the coupon d.c. current density $I_{d.c.}$ is obtained from equation (2).

Coupon a.c. current density, $I_{a.c.}$: Using coupon current $I(t)$ and coupon d.c. current density $I_{d.c.}$, the coupon a.c. current density $I_{a.c.}$ is obtained from equation (3).

Distortion factor, DF: The degree of the distortion of the obtained waveform compared to sine wave for a period of 50 Hz

E_{off} = **Fout!** (1)

$I_{d.c.}$ = **Fout!** · **Fout!** (2)

$I_{a.c.}$ = **Fout!** · **Fout!** (3)

DF = | [(coupon d.c. current density) – {(the maximum coupon current density) – |(the minimum coupon current density)|}／2]／{(the maximum coupon current density) – |(the minimum coupon current density)|} | for a period of 50 Hz (4)

where:

$E_{off}(t)$ = coupon potential after disconnecting the coupon from the pipe in each subunit
A = surface area of a coupon
$I(t)$ = coupon current at t ms in each subunit

3 Procedure for sound evaluation of the a.c. corrosion risk

The evaluation of a.c. corrosion likelihood was performed by evaluation of the following parameters on condition that coupon a.c. voltage was being lower than 15 V:

– coupon instant-off potential,
– coupon d.c. current density,
– coupon a.c. current density.

Procedure for sound evaluation of the a.c. corrosion risk was comprised of three processes:
1) calculation process;
2) extraction process;
3) specification process.

The first process was to calculate coupon instant-off potential E_{off}, coupon d.c. current density $I_{d.c.}$, and coupon a.c. current density $I_{a.c.}$.

Typical measuring period was an hour. Measuring period of an hour was comprised of 360 units that had all the same 10 second with the coupon/pipe on-state being 8,5 second and the coupon/pipe off-state being 1,5 second. Measurements were made by using a developed instrumentation by the authors [6].

A coupon/pipe on-state period consisted of 400 subunits. Each subunit was set to 20 millisecond that corresponded to a single period of 50 Hz. In each subunit, using coupon current measured at intervals of 0,1 millisecond and coupon d.c. current density $I_{d.c.}$ obtained from equation (2), coupon a.c. current density $I_{a.c.}$ was calculated from equation (3). Thus, a set of $I_{d.c.}$ and $I_{a.c.}$ was stored every subunits.

For a coupon/pipe on-state of 8 second, a total of 400 data on $I_{d.c.}$ and $I_{a.c.}$ were obtained. Coupon instant-off potential E_{off} was obtained from equation (1) by averaging a total of 200 coupon potentials between 80 and 100 millisecond after the coupon was disconnected from the pipe.

The second process was to extract the maximum coupon a.c. current density $I_{a.c.}^{max}$ from 400 coupon a.c. current densities $I_{a.c.}$ obtained from every units. A total of 360 data on the extracted maximum coupon a.c. current density $I_{a.c.}^{max}$ with its waveform, and coupon d.c. current density $I_{d.c.}$ obtained from the same subunit were stored.

The final process was to specify the extracted coupon a.c. current density $I_{a.c.}^{max}$ as affecting a.c. corrosion. The requirements to regard the coupon a.c. current density for a single period of 50 Hz as that affecting a.c. corrosion are:
1) polarity reversal;
2) consistency with commercial current frequency;
3) small distortion factor.

If the extracted $I_{a.c.}^{max}$ fulfilled the above mentioned requirements, $I_{a.c.}^{max}$ was symbolized by $I_{a.c.}^{max}(50Hz)$. Finally, a set of ($I_{d.c.}$, $I_{a.c.}^{max}(50Hz)$) was stored with the waveform of $I_{a.c.}^{max}(50Hz)$.

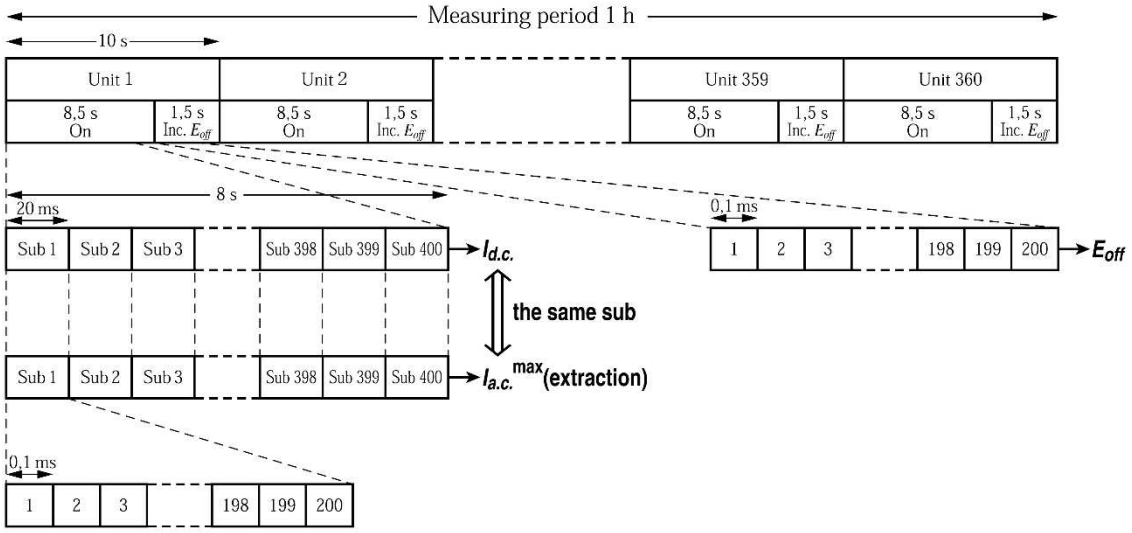

Key
Sub: subunit that has 20 millisecond (ms) for a single period of 50 Hz

Figure 1 — The schematic representation of measurement on coupon d.c. current densities $I_{d.c.}$, coupon a.c. current densities $I_{a.c.}^{max}$(50Hz), and coupon instant-off potentials E_{off} over 1 hour

4 Field study on the cathodically protected steel pipeline under a.c. interference

Field study was carried out on the cathodically protected steel pipeline under a.c. interference by the operation of a.c.-electrified railway system, to investigate the relationship between coupon a.c. current density and the a.c. corrosion risk, and to address a.c. corrosion process. The coupon was connected to the polyethylene coated 400 mm diameter gas pipeline paralleling a 25 kV a.c.-electrified railway system which operated at frequency of 50 Hz with great acceleration, high speed and long trains (250 m). The steel coupon was installed in the monitoring station where the a.c. current density reached its maximum. The a.c.-electrified railway system did not operate after midnight until early morning (around 0:00 - 6:00). High speed a.c. trains passed the monitoring station every several minutes at a speed of 150 to 200 kilometers per hour.

5 Results and discussion

5.1 Coupon instant-off potential and coupon d.c. and a.c. current densities

According to the above mentioned procedure in **3**, 350 ($I_{d.c.}$, $I_{a.c.}^{max}$(50Hz)) data were extracted out of a total of 360 ($I_{d.c.}$, $I_{a.c.}^{max}$) data.

Figure 2 shows the data on coupon instant-off potential E_{off}, coupon d.c. current density $I_{d.c.}$, and coupon a.c. current density $I_{a.c.}^{max}$(50Hz) over 1 hour in August 2014. The dotted line graph of $I_{a.c.}^{max}$(50Hz) in Figure 2 shows a broken line, indicating no data on $I_{a.c.}^{max}$(50Hz) in places.

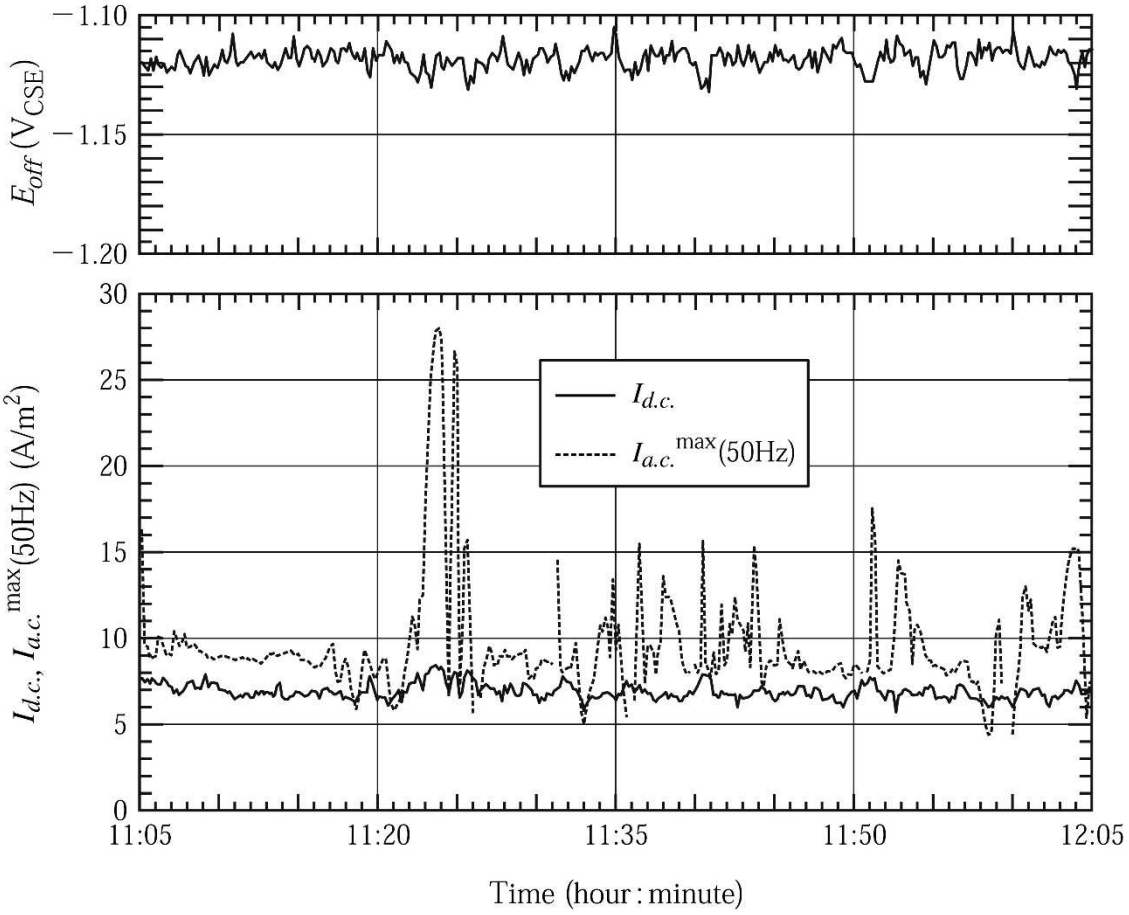

Figure 2 — The data on coupon instant-off potentials E_{off}, coupon d.c. current densities $I_{d.c.}$, and coupon a.c. current densities $I_{a.c.}^{max}$(50Hz) over 1 hour

The plot in Figure 3 illustrates correlation between the ratio of coupon a.c. current density $I_{a.c.}^{max}$(50Hz) to coupon d.c. current density $I_{d.c.}$ and $I_{a.c.}^{max}$(50Hz). It has been clarified that coupon a.c. current density $I_{a.c.}^{max}$(50Hz) increased with increasing $I_{a.c.}^{max}$(50Hz)/$I_{d.c.}$ proportionately with a correlation coefficient of 0,979. The slope of regression line was 0,814.

ISO/FDIS 18086 [8] explains that the ratio of a.c. current density to d.c. current density between 3 and 5 indicates a low risk of a.c. corrosion.

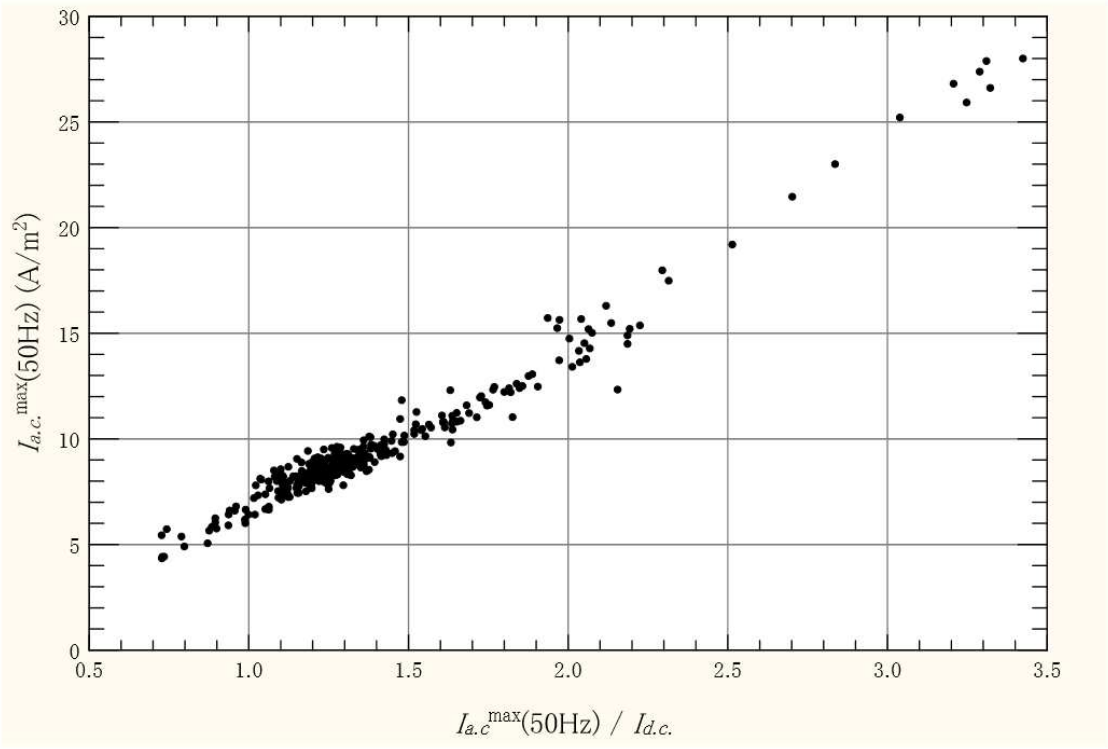

Figure 3 — Effect of the ratio of coupon a.c. current density $I_{a.c.}^{max}$(50Hz) to coupon d.c. current density $I_{d.c.}$ on coupon a.c. current density $I_{a.c.}^{max}$(50Hz)

Summary data are shown in Table 1.

Table 1 — Results of instant-off potential E_{off}, d.c. current density $I_{d.c.}$, and a.c. current density $I_{a.c.}$ at a coupon over 1 hour in August 2014

Coupon instant-off potential E_{off} (V_{CSE})	360 data	Average	−1,119
		Maximum	−1,105
		Minimum	−1,132
		Standard deviation	0,0044
Coupon d.c. current density $I_{d.c.}$ (A/m^2)	360 data	Average	6,888
		Maximum	8,423
		Minimum	5,719
		Standard deviation	0,453
Coupon a.c. current density $I_{a.c.}^{max}$(50Hz) (A/m^2)	350 data	Average	9,666
		Maximum	27,996
		Minimum	4,343
		Standard deviation	3,423
$I_{a.c.}^{max}$ (50Hz) /$I_{d.c.}$	350 data	Average	1,39
		Maximum	3,42
		Minimum	0,73
		Standard deviation	0,411

The evaluation of a.c. corrosion likelihood was done on the basis of ISO 15589-1 [9] and ISO/FDIS 18086 [8].

The results obtained from Figures 2 and 3, and Table 1 were as follows:

1) Coupon instant-off potential E_{off} was very stable between −1,132 and −1,105 V_{CSE} which satisfied ISO 15589-1. There was a small standard deviation of 0,0044.
2) There was significant variation between 4,343 and 27,996 A/m^2 in the $I_{a.c.}^{max}$(50Hz) that was the result of a.c.-electrified railway system loading changes. All of the data on $I_{a.c.}^{max}$(50Hz) for measuring period of 1 hour satisfied ISO/FDIS 18086.
3) Coupon d.c. current density $I_{d.c.}$, meanwhile, maintained stable values of 5,719 to 8,423 A/m^2 with very small standard deviation of 0,453 which was about one order smaller than that of $I_{a.c.}^{max}$(50Hz).
4) The ratio of $I_{a.c.}^{max}$(50Hz) to $I_{d.c.}$ was 0,73 to 3,42 less than 5, suggesting a low risk of a.c. corrosion.

The above-mentioned results shown in Figure 2 indicated that the pipeline had low risk of a.c. corrosion. The acceptable a.c. interference was fulfilled by point earthing where the pipeline crossed the overhead HVAC electric power line with a group of magnesium electrodes as earthing electrodes, and the installation of d.c. decoupling devices.

Owing to the use of a direct current power source to deliver an electrical current with a built-in high efficiency switching regulator equipped with pulse width module regulation, power factor of about 1, low ripple content etc. in impressed current cathodic protection system, coupon d.c. current densities $I_{d.c.}$ were relatively stable as shown in Figure 2.

5.2 Waveforms of $I_{a.c.}^{max}$(50Hz)

Figure 4 shows the typical four waveforms for a single period of 50 Hz over 1 hour in August 2014.Each $I_{a.c.}^{max}$(50Hz) is correspondence with unit number depicted in Figure 4.The data regarding the four waveforms are shown in Table 2.

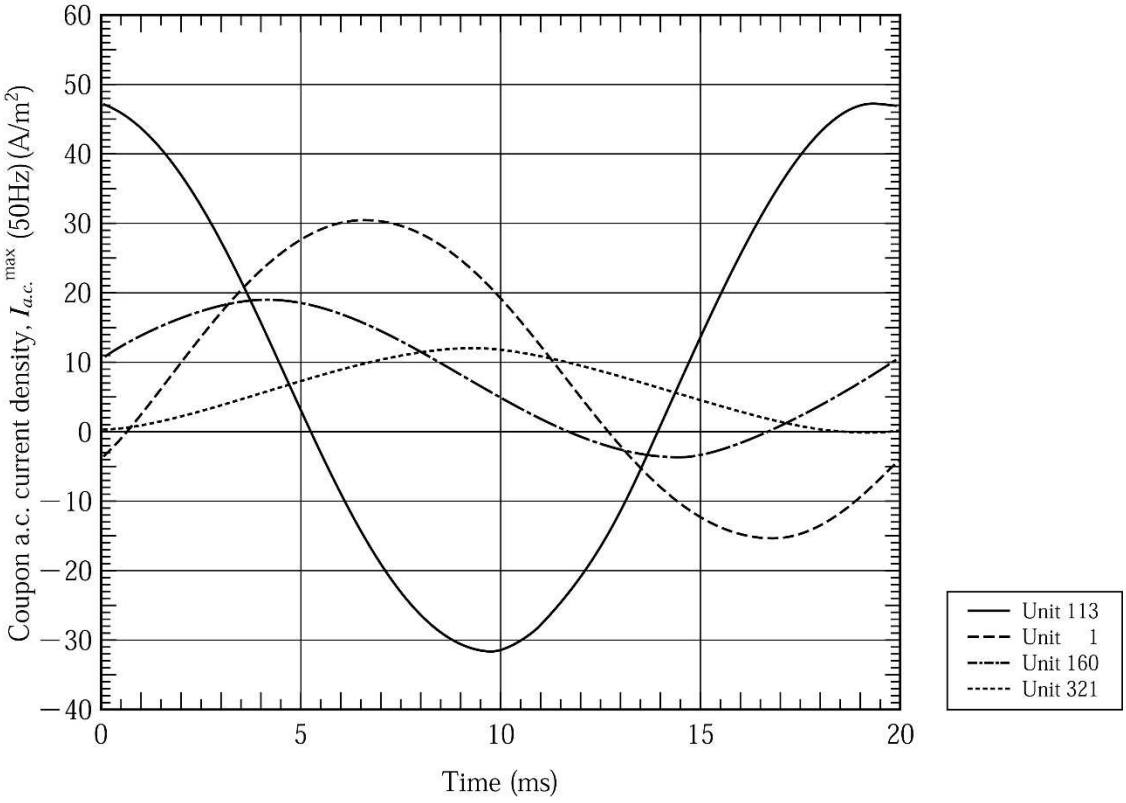

Figure 4 — The typical four waveforms for a single period of 50 Hz over 1 hour in August 2014

Table 2 — The data on the four waveforms for each unit

Parameter	Unit No			
	113	1	160	321
$I_{a.c.}^{max}$(50Hz) (A/m^2)	27,996	16,293	8,067	4,343
Peak value of anodic current in the waveform of $Ia.c.^{max}$(50Hz) (A/m^2)	–31,833	–15,417	–3,733	–0,200
Peak value of cathodic current in the waveform of $Ia.c.^{max}$(50Hz) (A/m^2)	47,350	30,667	19,083	12,083
Difference in appearance time between the maximum and the minimum values for $I_{a.c.}^{max}$(50Hz) (ms)	9,7	10,2	10,3	9,7
Distortion factor	0,0539	0,0083	0,0120	0,0040
Ratio of anodic current periods of time to 20 ms	0,435	0,250	0,259	0,035
$I_{d.c.}$ (A/m^2)	8,176	7,688	7,767	5,966
$I_{a.c.}^{max}$(50Hz) / $I_{d.c.}$	3,4	2,1	1,0	0,7

5.3 Analysis of data on $I_{a.c.}^{max}$(50Hz)

In 1967, Dévay et al. [10] showed that corrosion rates of iron in 5% KCl solution increased with increased a.c. current densities of 0 to 250 A/m^2 at different cathodic d.c. current densities of 0 to 10 A/m^2. More recently, Ormellese et al. [11] reported that corrosion rates of carbon steel specimens type API 5L X52 in sand containing solution saturated with sulfate and chloride ions increased with increased a.c. current densities of 1 to 500 A/m^2 at different cathodic current densities of 1,0 to 10 A/m^2 and a.c. current densities greater than 10 A/m^2 caused corrosion rates greater than 0,01 mm/y. These laboratory tests indicate that to clear the factors that influence higher a.c. current density at a constant d.c. current density can lead to the elucidation of the a.c. corrosion process.

The plot in Figure 5 illustrates correlation between the peak value of anodic current density and that of cathodic current density on $I_{a.c.}^{max}$(50Hz). The dotted line formed by the slope of −1 in Figure 5 shows the peak value of anodic current density is equal to that of cathodic on $I_{a.c.}^{max}$(50Hz), indicating symmetrical for the anodic and cathodic current density. The obtained solid line parallel to the dotted line showed that the magnitude of polarization in the cathodic direction was larger than in the anodic and the same extent of current peak shift in the anodic (negative) and cathodic (positive) directions took place.

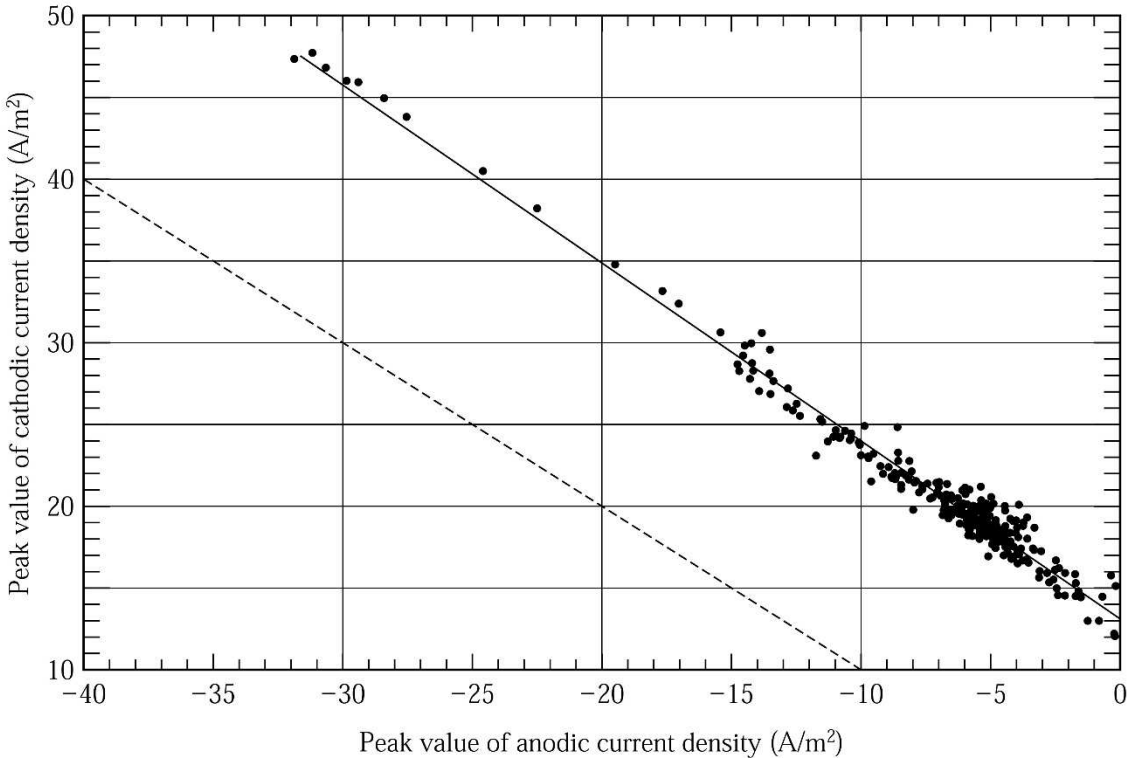

Figure 5 — Correlation between the peak value of anodic current density and that of cathodic current density on $I_{a.c.}^{max}$(50Hz)

It is important to seize as to which of anodic and cathodic current density affects $I_{a.c.}^{max}$(50Hz). Thereupon relationship between the ratio of the peak value of anodic current density to the peak value of cathodic current density and $I_{a.c.}^{max}$(50Hz) was

observed as shown in Figure 6. Figure 6 indicates that coupon a.c. current density $I_{a.c.}^{max}$(50Hz) increased with decreased the ratio of the peak value of anodic current density to the peak value of cathodic current density, suggesting that the contribution of anodic current density to $I_{a.c.}^{max}$(50Hz) was greater than that of cathodic current density.

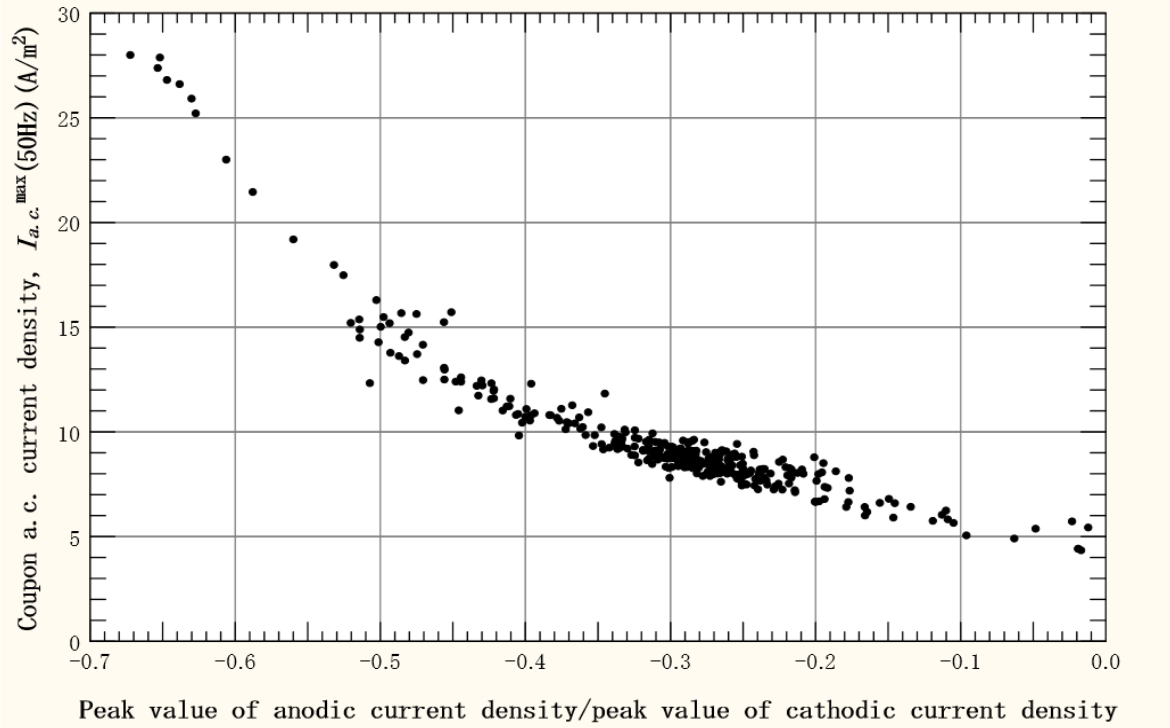

Figure 6 — Relationship between the ratio of the peak value of anodic current density to the peak value of cathodic current density and coupon a.c. current density $I_{a.c.}^{max}$(50Hz)

Furthermore, to understand the contribution of anodic current density solely to coupon a.c. current density $I_{a.c.}^{max}$(50Hz), correlation between the actual observed peak value of anodic current density for a single period of 50 Hz and coupon a.c. current density $I_{a.c.}^{max}$(50Hz) was analyzed. Here it can been seen that $I_{a.c.}^{max}$(50Hz) depended directly on the peak value of anodic current density. The result of the analysis, shown in Figure 7, indicates that coupon a.c. current density $I_{a.c.}^{max}$(50Hz) increased in inverse proportion to the peak value of anodic current density. Correlation coefficient was –0,996. The calculated slope of the regression line was –0,738, in good agreement with the theoretical value of –0,707 provided by the following speculation.

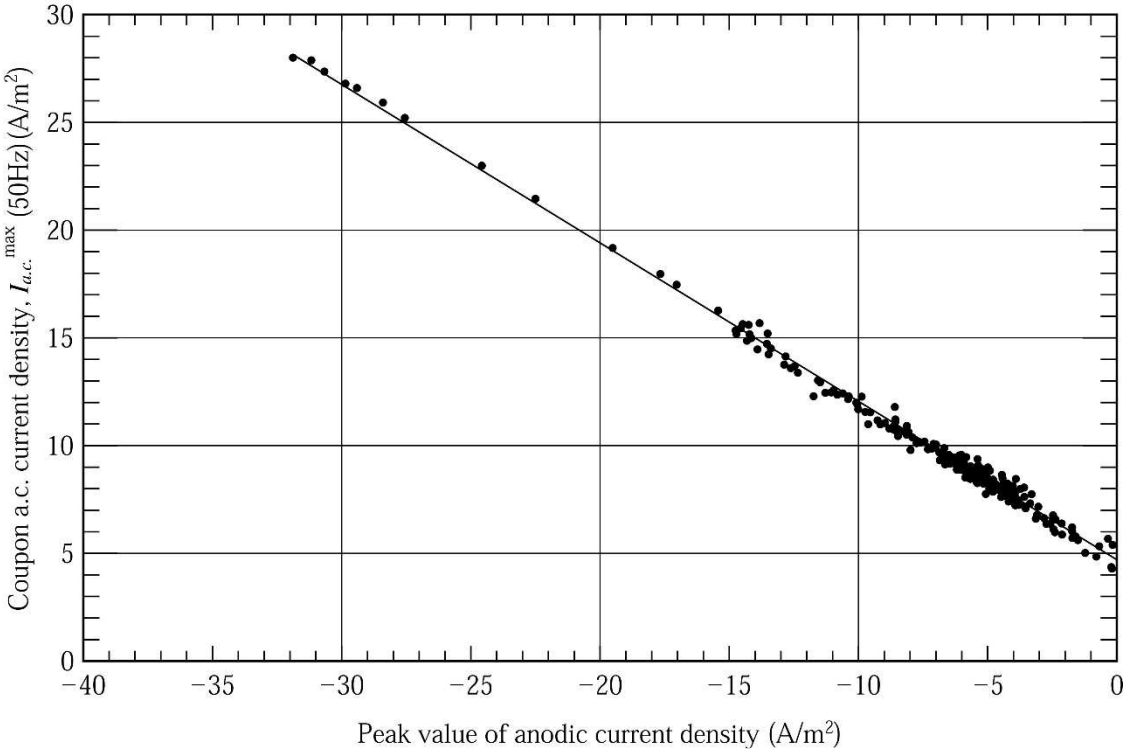

Figure 7 — Effect of the peak value of anodic current density on the coupon current density $I_{a.c.}^{max}$(50Hz)

As mentioned earlier, it should be noted that coupon d.c. current density $I_{d.c.}$ was relatively constant, and the magnitude of peak shift in anodic current density was equal to that of the cathodic if $I_{a.c.}^{max}$(50Hz) varies with time.

On the assumption that the maximum of coupon a.c. current density varies from Y to (Y+ΔY) as shown by the dotted line in Figure 8, the ratio of the peak value of anodic current density to that of cathodic is obtained as follows:
The ratio of the peak value of anodic current density to the peak value of cathodic current density
= **Fout!**
= **Fout!** · **Fout!** < **Fout!** ∵ $I_{d.c.}$+ Y > $I_{d.c.}$ – Y
The values of $I_{d.c.}$, Y, and ΔY are positive.

Therefore, if coupon a.c. current density $I_{a.c.}^{max}$(50Hz) increases, the ratio of the peak value of anodic current density to that of cathodic current density decreases.

When the maximum of coupon a.c. current density $I_{a.c.}^{max}$(50Hz) increases by ΔY as shown by the dotted line in Figure 8, coupon a.c. current density $I_{a.c.}^{max}$(50Hz) varies from Y/$\sqrt{,2}$ to (Y+ΔY) /$\sqrt{,2}$ .The slope of the straight line was –1/$\sqrt{,2}$ (–0,707). This is the reason why the slope of the regression line –0,738 in Figure 7 was considered to be consistent with –0,707.

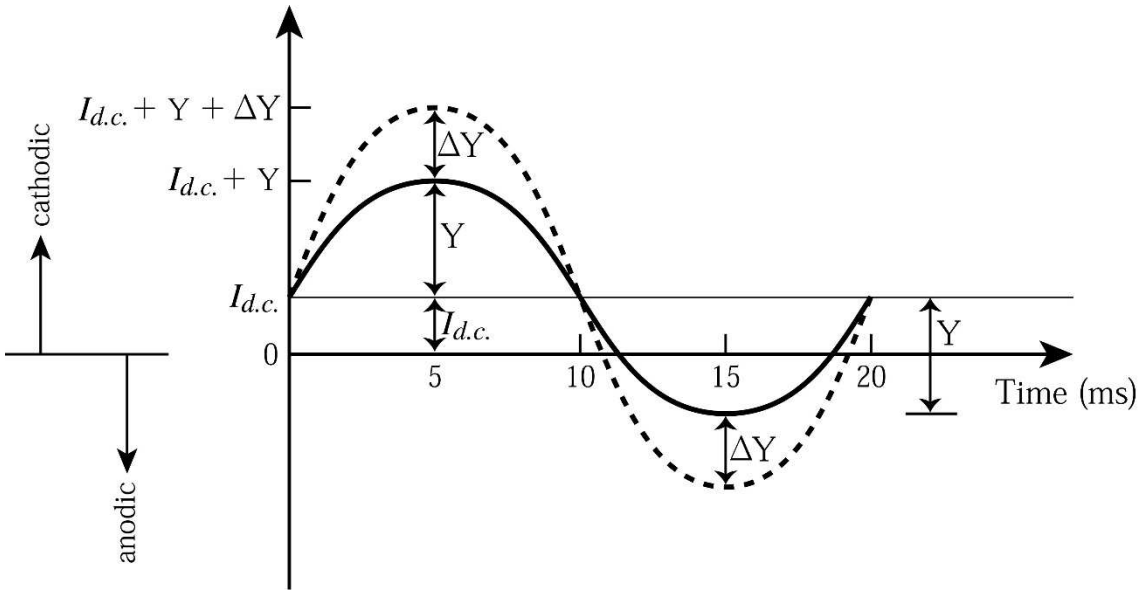

Figure 8 — Illustration of the increase in coupon a.c. current density

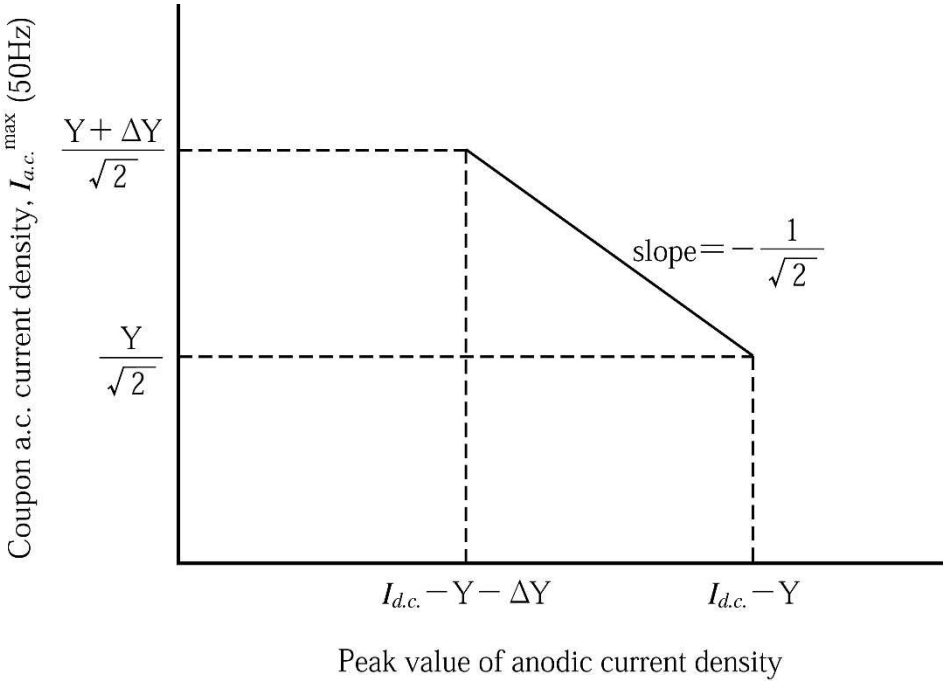

Figure 9 — Illustration of relationship between the decrease in peak value of anodic current density (the increase in absolute peal value of anodic current density) and the increase in coupon a.c. current density $I_{a.c.}^{max}$(50Hz) corresponding to Figure 8

It was proved that the peak of anodic current density was a critical parameter for

determining $I_{a.c.}^{max}$(50Hz). Furthermore, the effect of anodic current periods of time on the coupon a.c. current density $I_{a.c.}^{max}$(50Hz) was studied. Effect of the ratio of anodic current periods of time to 20 ms (a single period of 50 Hz) on the coupon a.c. current density $I_{a.c.}^{max}$(50Hz) is shown in Figure 10, suggesting that the coupon a.c. current density $I_{a.c.}^{max}$(50Hz) was also largely dependent on the magnitude of anodic current periods of time for a single period of 50 Hz.

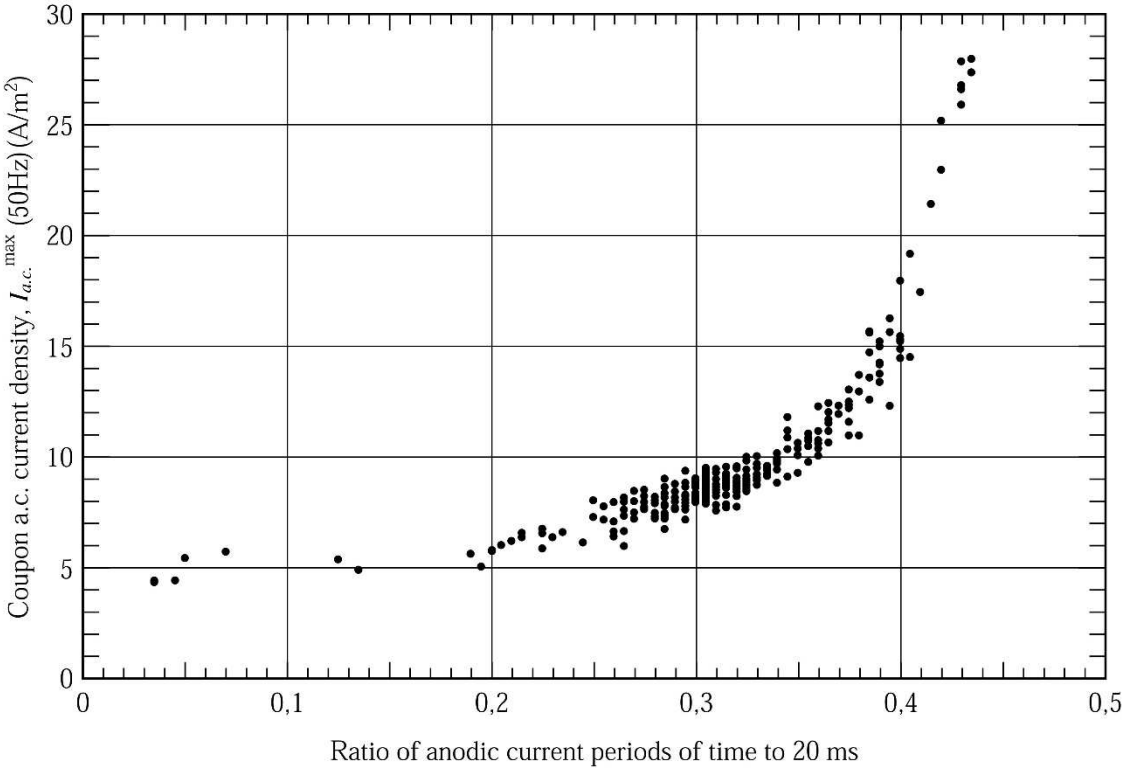

Figure 10 — Effect of the ratio of anodic current periods of time to 20 ms on the coupon a.c. current density $I_{a.c.}^{max}$(50Hz)

The following results were obtained.

The greater the ratio of anodic periods of time to 20 millisecond (ms), higher coupon a.c. current density $I_{a.c.}^{max}$(50Hz). By taking Figure 7 into account, longer anodic current periods of time with higher peak value of anodic current density for a single period of 50 Hz can cause higher a.c. corrosion rate. This result was thought to be closely related with the steel corrosion.

5.4 Proposal of a.c. corrosion process

The process of a.c. corrosion may involve anodic and cathodic reactions. The existence of anodic and cathodic currents is proof that the oxidations and reduction reactions occurred by their currents on the same surface. During the anodic current period of time the steel surface is oxidized by the anodic current according to reaction (5), resulting in the formation of the passive film Fe_3O_4. Subsequently during the cathodic current periods of time the passive film is cathodically polarized presumably by reaction (6), leading to the destruction of passivity by the reduction of the passive

film.

$$3Fe + 8OH^- \rightarrow Fe_3O_4 + 4H_2O + 8e^- \quad (5)$$

$$Fe_3O_4 + 8H^+ + 2e^- \rightarrow 3Fe^{2+} + 4H_2O \quad (6)$$

After that, the repetition of irreversible anodic and cathodic currents roughen the steel surface, resulting in corrosion at the steel-electrolyte interface by reaction (7). Physical exfoliation could be a possible explanation of the solid substrate breakdown, leading to the steel dissolution.

$$Fe \rightarrow Fe^{2+} + 2e^- \quad (7)$$

If the steel that itself appears at very alkaline pH, the dissolved $HFeO_2^-$ is formed according to the anodic reaction (8), leading to cause steel corrosion.

$$Fe + 2H_2O \rightarrow HFeO_2^- + 3H^+ + 2e^- \quad (8)$$

Figure 11 shows the Pourbaix diagram for iron [12]. It should be noted that the coupon instant-off potential of –1,1 V_{CSE} obtained from this field study was at a potential below the equilibrium potential for the hydrogen evolution reaction at pH's below about 13.

From the thermodynamic point of view, potential oscillations between immunity (Fe) and passivity (Fe_3O_4) domains at very alkaline pH of Pourbaix diagram (Figure 11, ③ line) may cause corrosion as the result of the destruction of passivity by the cathodic reaction (6) and the formation of dissolved $HFeO_2^-$ by the anodic reaction (8).

Taking the process into account, polarity reversal in coupon current for a single period can be linked with the a.c. corrosion likelihood. As seen in Figure 4, the existence of anodic and cathodic currents is proof that anodic and cathodic reactions occurred. The results and speculation are applicable at commercial current frequencies (such as 16 ⅔, 50 or 60 Hz).

Based on the above-mentioned speculation, the requirements to regard the coupon a.c. current density for a single period of commercial current frequency as that affecting a.c. corrosion are:

1) polarity reversal;
2) consistency with commercial current frequency;
3) small distortion factor.

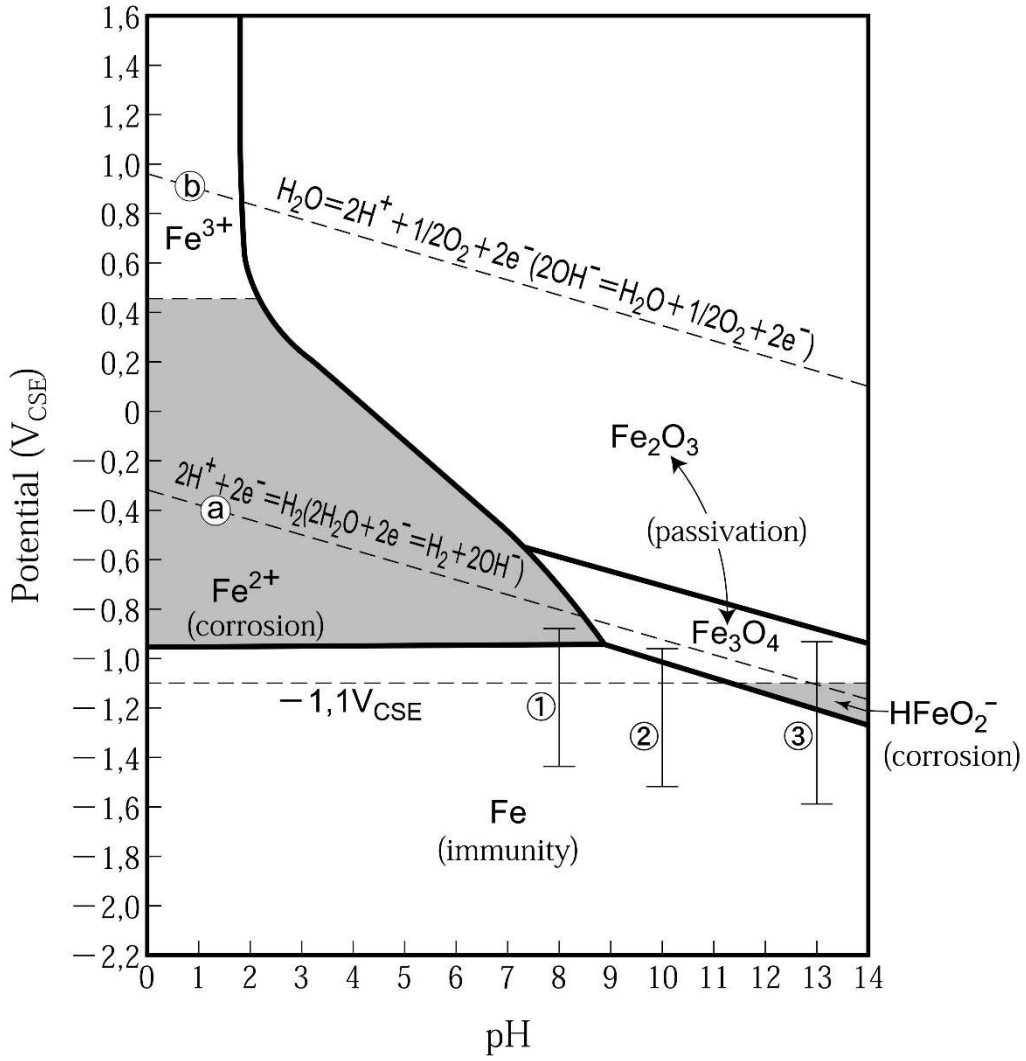

Figure 11 — Pourbaix diagram for iron

6 Conclusions

Based on the field study of the cathodically protected steel pipeline under a.c. interference by a.c.-electrified rail system which operated at frequency at 50 Hz, the following conclusions were made.

— Procedure for sound evaluation of the a.c. corrosion risk was developed.
— It is very important to ascertain that the coupon a.c. current density is that affects a.c. corrosion at 50 Hz.
The requirements to regard the coupon a.c. current density for a single period of 50 Hz as affecting a.c. corrosion are:
1) polarity reversal;
2) consistency with 50 Hz;
3) small distortion factor of a waveform.
— Longer anodic current periods of time with higher peak value of anodic current density for a single period of 50 Hz can cause higher a.c. corrosion rate.

References

[1] A. Pourbaix, P. Carpentiers, R. Gregoor, “Detection and assessment of alternating current corrosion,” Materials Performance, 39, 3, pp.34-37 (2000)

[2] A. Poubaix, P. Carpentiers, “Measurement and analysis of AC induced corrosion,”CEOCOR International Congress, Paper 2013-34, Florence, Italy (2013)

[3] P. Hartmann, “Außenkorrosionen an einer kathodisch geschützten Gasfern-leitung durch 50 Hz-Wechselstrombeeinflussung,” 3R international 30, 10, pp.584-589 (1991)

[4] D. Funk, W. Prinz, H.-G. Schöneich, “Untersuchungen zur Wechselstromkorrosion an kathodisch geschützten Leitungen,” 3R international, 31, 6, pp. 3-8 (1992)

[5] W. Prinz, “AC-Induced Corrosion on Cathodically Protected Pipelines,” UK CORROSION ’92, pp. 1-17 (1992)

[6] F. Kajiyama, Y. Nakamura, “Development of an advanced instrumentation for assessing the AC corrosion risk of buried pipelines,” CORROSION 2010, NACE International, Paper No. 10104 (2010)

[7] F. Kajiyama, “Requirements of Coupon AC Current Density Affecting AC Corrosion of Buried Steel Pipelines,” CORROSION 2015, NACE International, Paper No. 5594 (2015)

[8] ISO/FDIS 18086 Corrosion of metals and alloys — Determination of AC corrosion — Protection criteria (2014)

[9] ISO 15589-1 Petroleum and natural gas industries — Cathodic protection of pipeline transportation systems —Part 1: On-land pipelines (2003)

[10] J. Dévay, S. S. Abd El-Rehim, V. Takács, “Electrolytic A.C. Corrosion of Iron,” Acta Chimica Academiae Scientiarum Hungaricae Tomus, 52 (1), pp.63-68 (1967)

[11] M. Ormellese, A. Brenna, L. Lazzari, “AC Corrosion of Cathodically Protected Buried Pipelines：Critical Interference Values and Protection Criteria,” CORROSION 2015, Paper No. 5753 (2015)

[12] M. Pourbaix, “Atlas of electrochemical equilibria in aqueous solutions,” National Association of Corrosion Engineers (1966)